Cosmic Rays During the Recent Unusual Solar minimum

Lingling Zhao

Center for Space Science and Applied Research, Chinese Academy of Sciences

April 21, 2011

Outline

Introduction

- Observation
  Intensity of Galactic cosmic rays (GCRs) measured during the recent solar minimum was the highest ever recorded. We studied CRs data on spacecrafts near the Earth and ground-based neutron monitors, which indicate that the modulation of CRs is not dominated by the mechanism of particle drift through current sheet during this $A < 0$ cycle as we normally think.
- Modulation
  We use a model of GCRs transport in the three-dimensional heliosphere based on a simulation of Markov stochastic process to study the possible reasons. Our preliminary results show that it is due to the weaker Interplanetary magnetic field and lower perpendicular diffusion coefficient.

Brief introduction to GCR

- Solar magnetic field

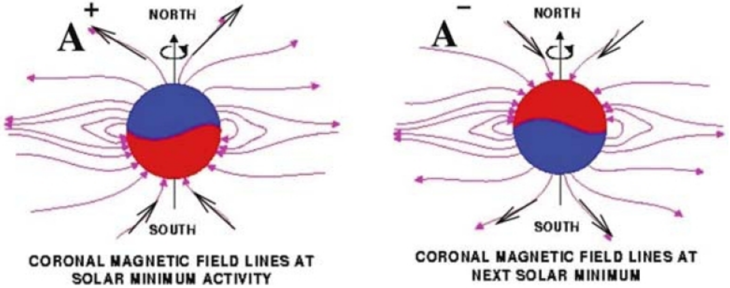

- A^+ are times when the solar magnetic field is directed outward from the sun in the northern polar and inward in the southern polar region.

Brief introduction to GCR

- Transport through a wavy current sheet

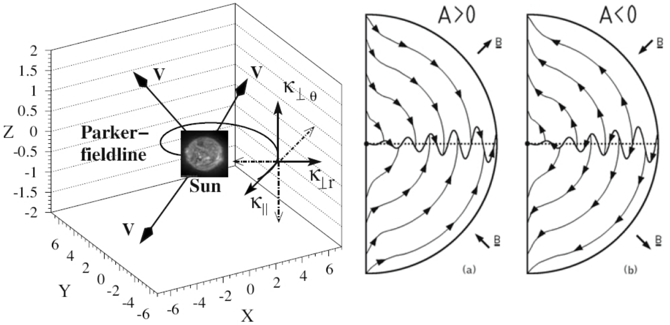

- Diffusion with respect to the Parker spiral (left). The global drift pattern of positively charged particles in $A > 0$ and $A < 0$ solar magnetic epoch (right).

Brief introduction to GCR

- Solar modulation of GCRs

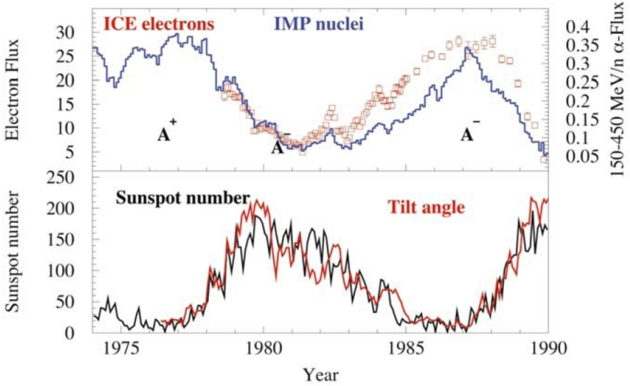

- Both helium and electrons vary in anti-correlation with 11-year solar activity cycle. In the $A < 0$, the time profiles of positively charged particles peaked, whereas they were more or less flat in $A > 0$.

Neutron monitor

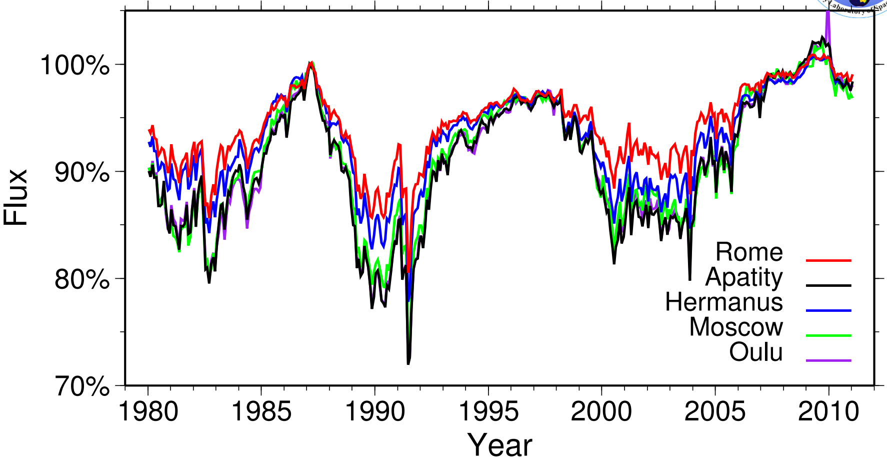

Figure 1: monthly mean rates for NMs from 1980.01 to 2011.01; rates are normalized to 100% for February of 1987.

Rigidity of NMs

- Rome 6.27Gv
- Apatity 5.6Gv
- Hermanus 4.58Gv
- Moscow 2.43Gv
- Oulu 0.8Gv
- Jungfraujoch 4.49Gv
- Climax 3Gv
- Kiel 2.36Gv
- Magadan 2.09Gv

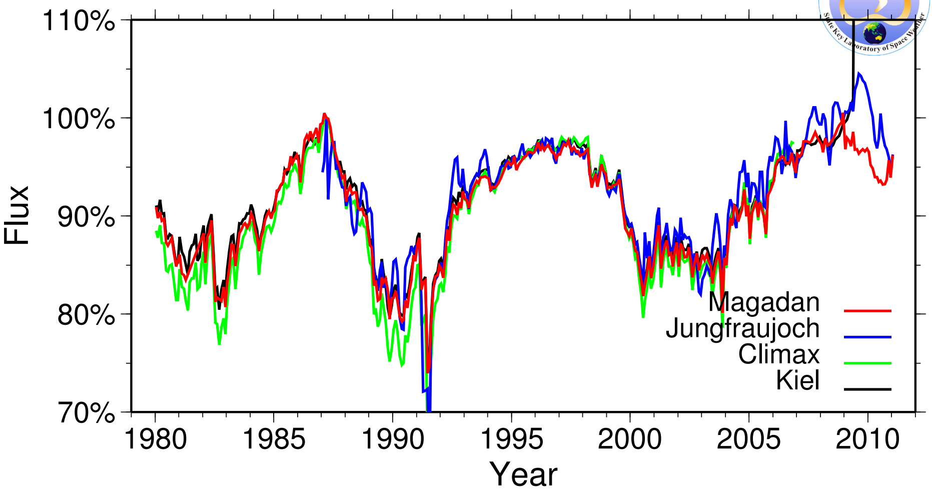

Figure 2: rates are normalized to 100% for March of 1987

Heavy ions on the ACE

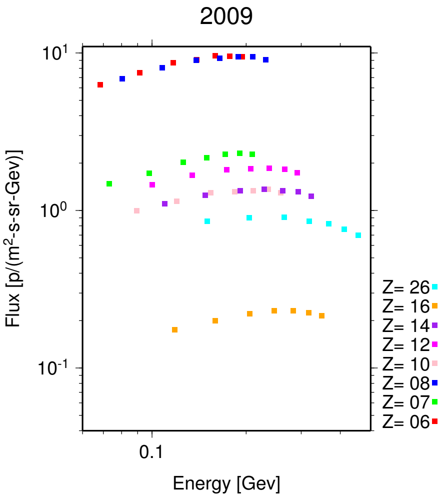

- The number is the proton number of partilce, they are C,N,O,Ne,Na,Mg,Si,S,Fe.
- I use annual mean hourly rates data, this is the solar minimum of cycle 24(2009).
- Each ion has seven energy ranges. We calculation annual deviation to study.

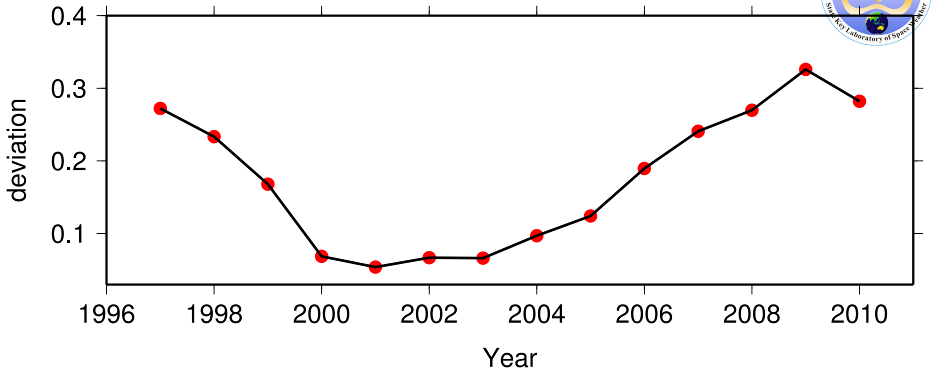

Figure 3: We calculate deviation every year for all heavy ions, $\sqrt{\frac{(C-\bar{C})^2}{N}}$. The deviation vary in anti-correlation with 11-year solar activity cycle. And the deviation in 24 solar cycle is much bigger and sharp than the one in 23 solar cycle.

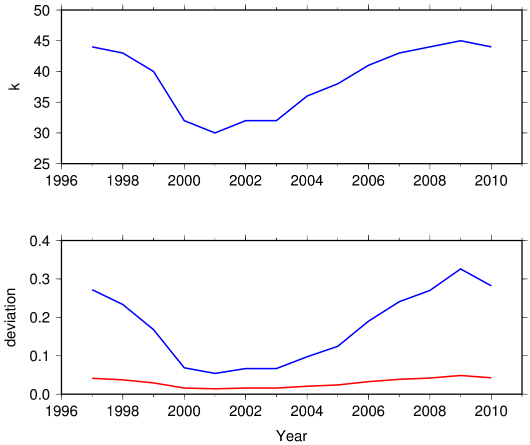

Figure 4: top:action; bottom:deviation compare

- We calculate annual deviation for all particles (5-28) from 1997 to 2010(blue line in bottom panel)
- We use $f' = T(z)f$ to concentrate flux of all particles together.

$$T(z) = 10^{k(z-z_0)} \qquad (1)$$

- Deviation after processing is the red line in bottom panel. It is much smaller comparing with before.

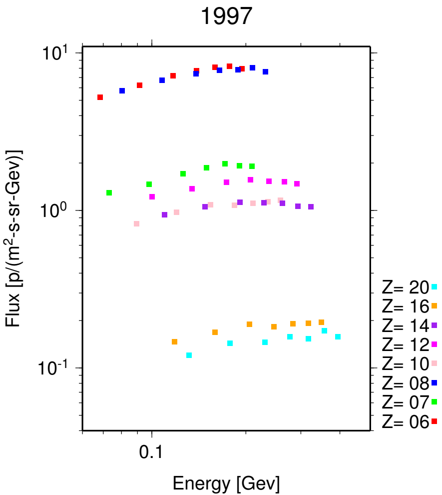

Figure 5: flux before processing in the solar minimum 23

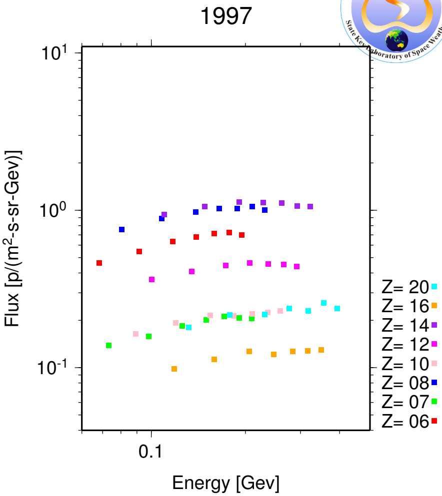

Figure 6: flux after processing

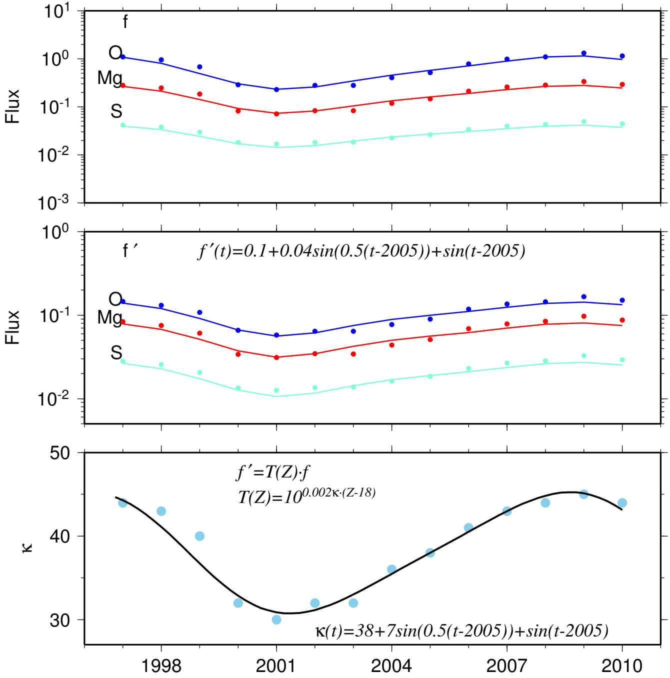
f
O
Mg
S
Flux
f ′
$f'(t)=0.1+0.04\sin(0.5(t-2005))+\sin(t-2005)$
$f'=T(Z)\cdot f$
$T(Z)=10^{0.002\kappa\cdot(Z-18)}$
$\kappa(t)=38+7\sin(0.5(t-2005))+\sin(t-2005)$
κ
1998
2001
2004
2007
2010

Deviation for all ions

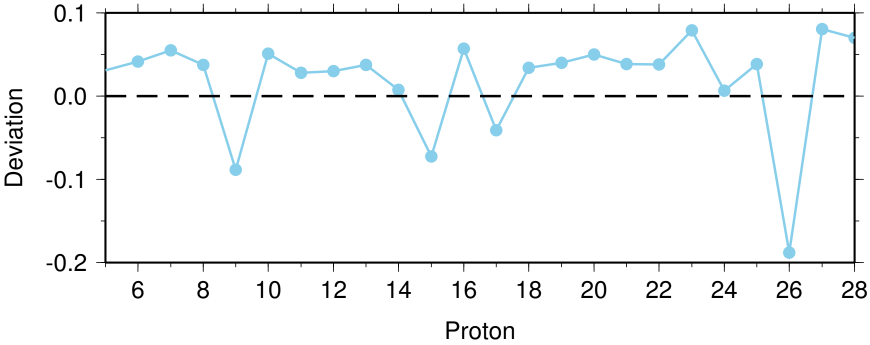

Figure 7: We calculate relative deviation between our modulated results and the observation for all elements. $D = \sqrt{\frac{\sum_{year}(\frac{f_m - f_o}{f_o})^2}{years}}$. Except iron and some rare ions our modulation fit observation well.

Ulysses trace

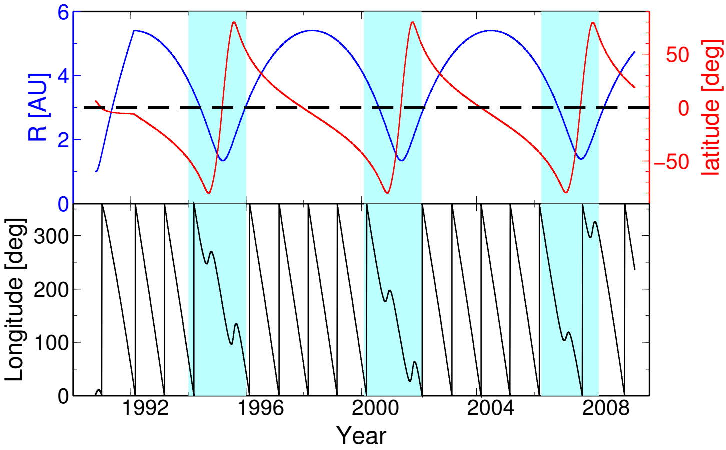

Figure 8: Three Ulysses fast latitude scans:first and third take place at solar minimum and second one under solar maximum.

Proton on the Ulysses

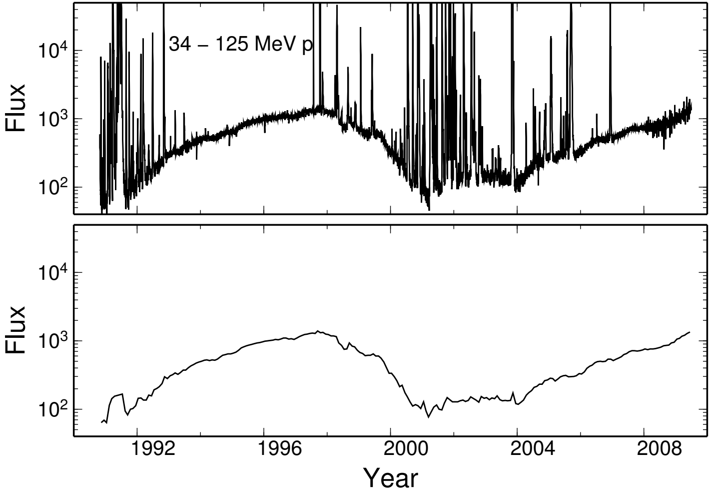

Figure 9: From top to bottom are shown the daily averaged flux of 38-125 Mev protons from 1990 to 2009 and the monthly averaged after data processing.

Proton on the IMP-8

- Monthly averaged data of 400Mev proton on the IMP-8 after dealing.
- The energy of Proton on the IMP-8 is from 70Mev to 400Mev, time is from 1980 to 2001.

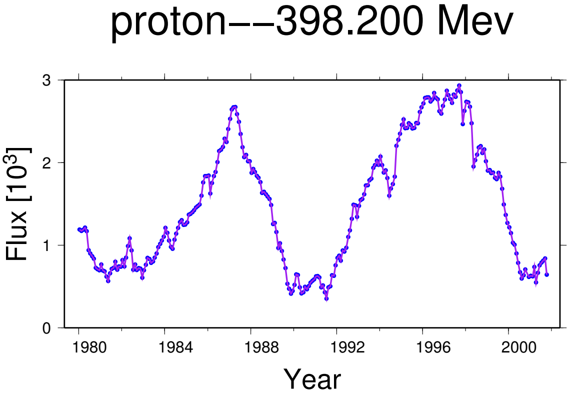

Figure 10: Monthly averaged after dealing

Pronton on the voyager1

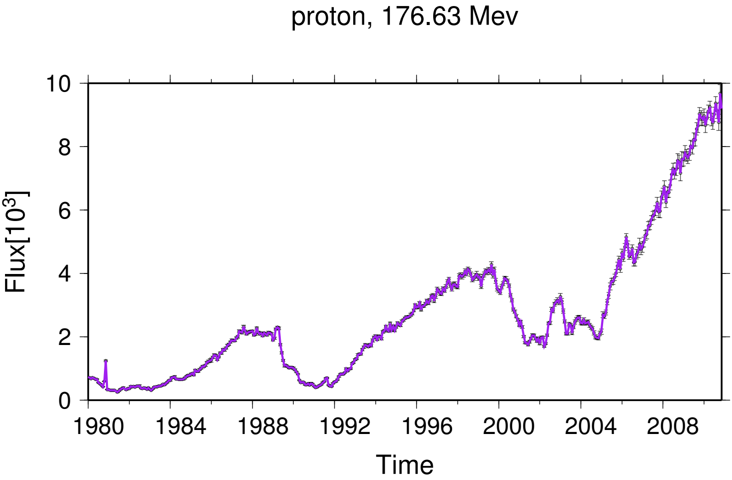

Figure 11: Daily averaged data of 176Mev proton on voyager1, available energy is from 22Mev to 176Mev.

Voyager1 trace

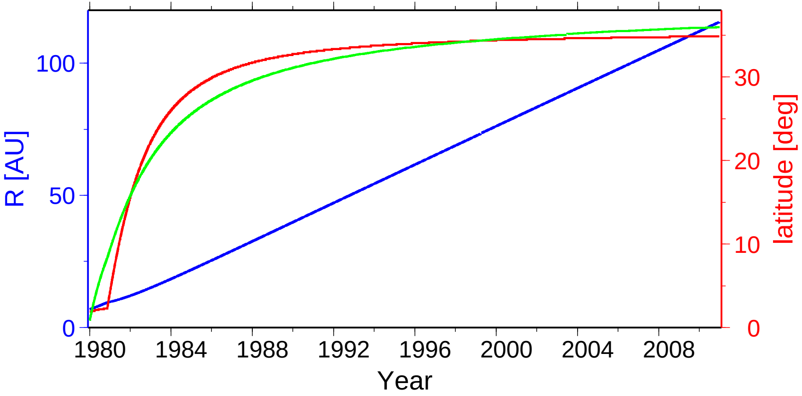

Figure 12: blue:radius, red:latitude, green:longitude

Fokker-Planck transport equation

Fokker-Planck equation

$$\frac{\partial f}{\partial t} = -(V + V_d) \cdot \nabla f + \nabla \cdot (\kappa \cdot \nabla f) + \frac{p}{3}(\nabla \cdot V)\frac{\partial f}{\partial p} \quad (2)$$

with

1. Drift speed:

$$V_{dr} = \frac{V_p p}{3q} \nabla \times \frac{B}{B^2} \quad (3)$$

2. Diffusion coefficient:

$$\kappa_{\parallel} = \kappa_{\parallel 0} \beta \left(\frac{p}{p_0} \right)^{b_{\parallel}} \left(\frac{B_e}{B} \right)^{a_{\parallel}} \quad (4)$$

$$\kappa_{\perp} = \kappa_{\perp 0} \beta \left(\frac{p}{p_0} \right)^{b_{\perp}} \left(\frac{B_e}{B} \right)^{a_{\perp}} \quad (5)$$

Calculation of wavy CS

- The current sheet

$$\theta_0 = \frac{\pi}{2} + \alpha \sin\left(\phi + \frac{r\Omega}{V_w}\right) \tag{6}$$

- calculation of IMF

$$B = \frac{A}{r^2}(\hat{e}_r - \Gamma e_\phi)\left[1 - 2H(\theta - \theta_0)\right] \tag{7}$$

- drift of wavy CS

$$v_{cs} = \frac{v}{6}\cos\alpha \frac{\triangle\theta_{cs}}{\sin(\alpha + \triangle\theta_{cs})} \tag{8}$$

with

$$\triangle\theta_{cs} = P/(80\cos\alpha) \tag{9}$$

Stochastic differential equation

We use Markov stochastic process to solve the transport equation, $X(s)$, $Y(s)$,$Z(s)$,$P(s)$ are time-backward stochastic processes described by ($U = V + V_d$)

$$\mathrm{d}x = \left(\frac{\partial \kappa_\perp}{\partial x} - U_x\right) \mathrm{d}s + \sqrt{2\kappa_\perp}\,\mathrm{d}W_x(s) \tag{10}$$

$$\mathrm{d}y = \left(\frac{\partial \kappa_\perp}{\partial y} - U_y\right) \mathrm{d}s + \sqrt{2\kappa_\perp}\,\mathrm{d}W_y(s) \tag{11}$$

$$\mathrm{d}z = \left(\frac{\partial \kappa_\parallel}{\partial z} - U_z\right) \mathrm{d}s + \sqrt{2\kappa_\parallel}\,\mathrm{d}W_z(s) \tag{12}$$

$$\mathrm{d}p = \frac{p}{3}\left(\nabla \cdot V\right) \mathrm{d}s \tag{13}$$

$$f(x, y, z, p, t) = \left\langle \int_0^t Q\left(X(s), Y(s), Z(s), P(s), s\right) \mathrm{d}s \right\rangle \tag{14}$$

Sample trajectory for $qA < 0$

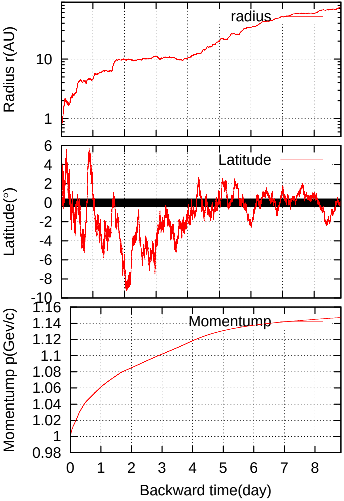

- A simulated stochastic process with Magnetic field polarity $qA < 0$.
- The radial distance, latitude, and momentum of the simulated particle are shown as functions of backward time S.
- The process starts at 1AU in the equatorial with $1 GeVc^{-1}$ momentum and runs backward in time until it exits at 75 AU.

Latitude-longitude distribution

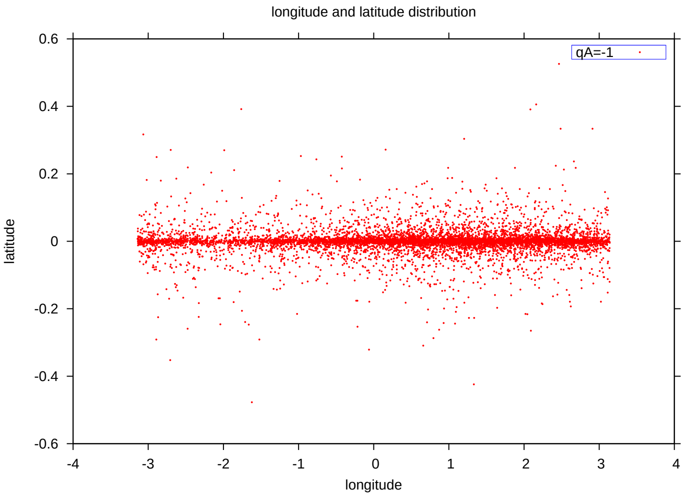

Figure 14: Latitude-longitude distribution of test particles for $qA < 0$.

Sample trajectory for $qA > 0$

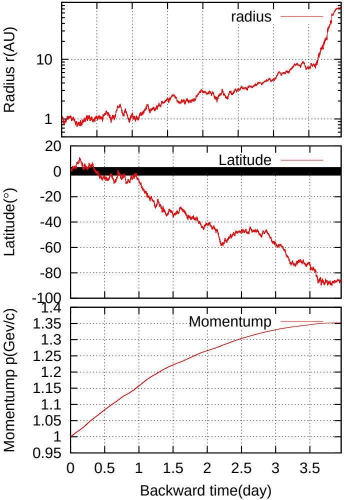

- The same as figure 1, but for $qA > 0$
- We note that the particle gains more momentum than in the case of qA negative.

Latitude-longitude distribution

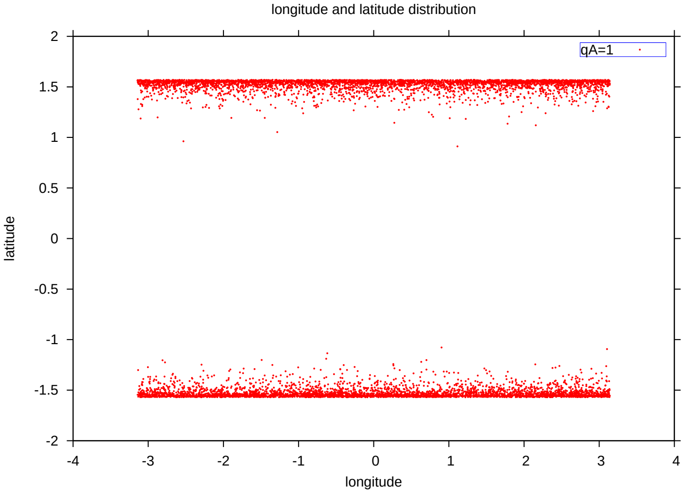

Figure 15: Latitude-longitude distribution of test particles for $qA < 0$.

Flux variation with Energy

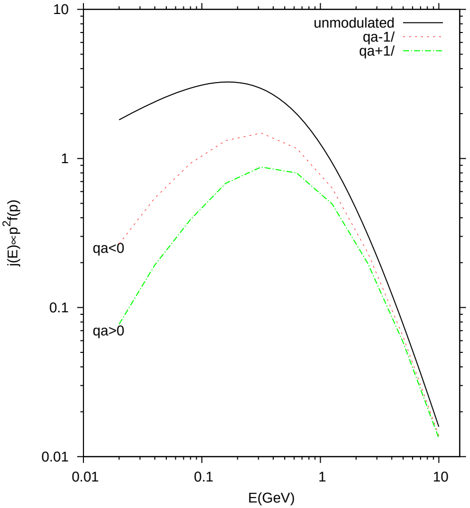

Figure 16: Ideal model

Modulation of TA

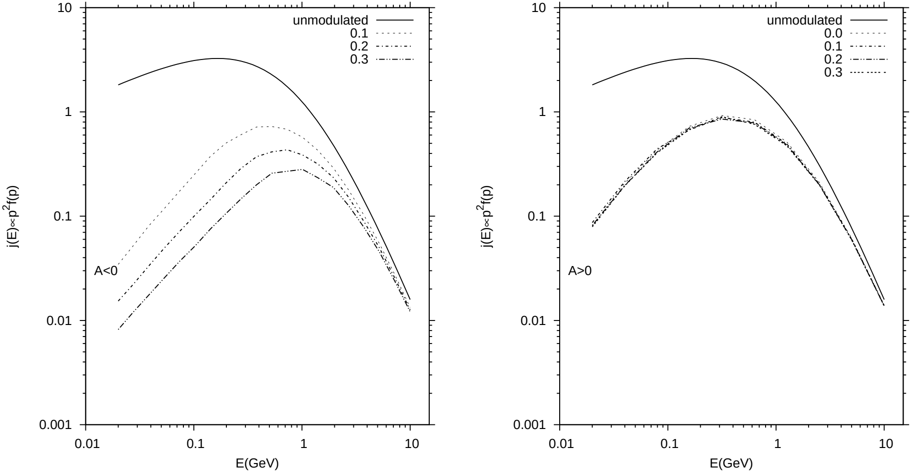

Transport parameter

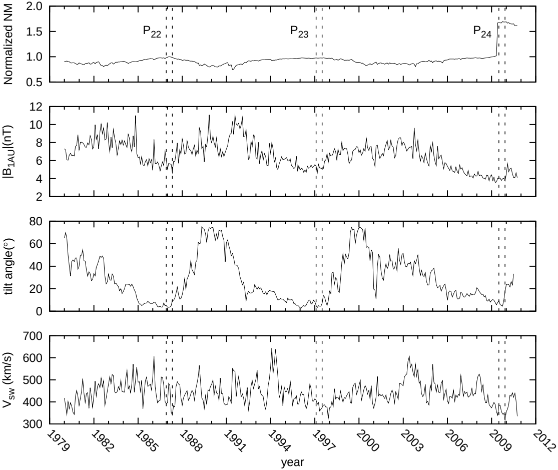

Figure 17: We use transport parameters carrying out a half year average

Ulysses modulation

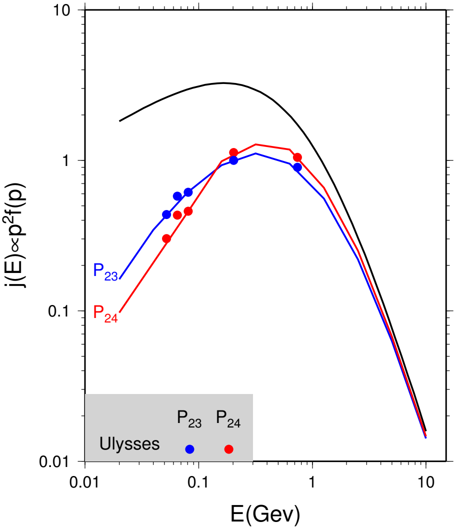

- We model proton intensity according to Ulysses trace
- Observation circles are obtained from Ulysses COSPIN.

Modulation result

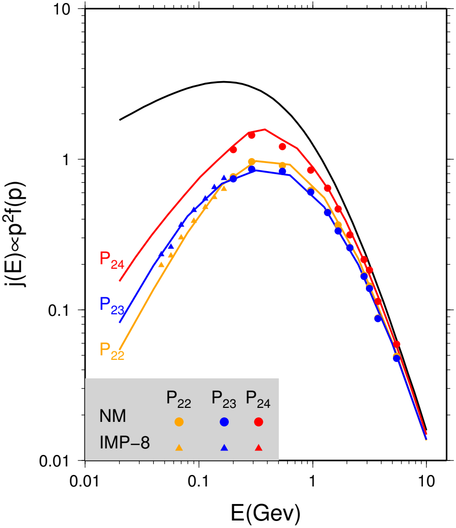

- We use transport parameters carrying out a half year average of each interval in our model of each solar minima.
- The observation data are obtained from neutron monitor and IMP-8.